Journal of Materials Chemistry C

ROYAL SOCIETY OF CHEMISTRY

COMMUNICATION

View Article Online
View Journal | View Issue



Cite this: J. Mater. Chem. C, 2024, 12, 9571

Received 25th April 2024,
Accepted 14th June 2024

DOI: 10.1039/d4tc01698j

rsc.li/materials-c

# Enhanced nonlinear optical properties of $Au_{25}$ nanocluster oligomers linked by bidentate dithiol†

Patryk Obstarczyk,[a] Julia Osmólska,[a] Michał Swierczewski,[b] Thomas Bürgi,[b] Marek Samoć[a] and Joanna Olesiak-Bańska *[a]

**Atomically-precise gold nanoclusters covered with thiol ligands are attractive candidates for advanced photonics, sensing and bioimaging applications. We show that covalent linking of $Au_{25}(PET)_{18}$ (PET – phenylethylmercaptan) with (1*R*,1′*R*)-6,6′-(1,4-phenylene)di-1,1′-binaphthyl-2,2′-dithiol (diBINAS) may offer a pathway towards atomically-precise materials with enhanced nonlinear optical properties. Interestingly, nanocluster oligomerization leads to moderate modification of the linear optical properties, but has a significant impact on their two-photon absorption performance. Two photon absorption cross-sections $\sigma_2$ of the monomers, dimers and trimers were measured *via* the z-scan technique in a wide range of wavelengths. The relative values of $\sigma_2$ are different from a simple additive scheme, *i.e.* in the resonance region the $\sigma_2$ enhancement is equal to factors of ~4 and ~8 for the dimer and trimer, respectively. In the off-resonance spectral region, the trimers exhibit 4 times higher two-photon absorption cross-section values than the monomers, while the dimers are characterized by enhancement factors slightly larger than 2.**



## Introduction

Controlled assembly of microscale and macroscopic materials from molecules and nanosized objects is of great importance for molecular electronics, advanced photonics, sensing, telecommunications and other technological applications.[1] Often, a specific building blocks assembly may result in the emergence of unique physicochemical properties, which cannot be attained by modifying the superstructure's building blocks alone. For example, plasmonic gold nanoparticles assembled into well-controlled aggregates exhibit new optical properties, *e.g.* plasmon band shifts, circular dichroism activity and the emergence of strongly coupled plasmon-exciton mixed states.[2] However, mastery over nano-sized building block organization within superstructures – ergo control over system functionality – is still challenging and has been attracting ever growing attention.[3]

While a variety of distinctive types of nano-objects can be obtained, atomically-precise gold nanoclusters (GNCs) are unique due to their physicochemical properties directly correlated with the number of gold atoms.[4] Their strictly defined structure and size places them on the bridge between molecular and metal-like structures,[5] which makes them perfect building blocks for functional superstructures with programmable properties.[6] Recently, a variety of experimental protocols based on dithiol linkers (*e.g.* benzene-1,4-dithiol) were used to prepare and then separate covalently linked aggregates of atomically-precise GNCs (*e.g.* $Au_{25}(SR)_{18}$ [SR: thiolate: phenylethane thiol or butanethiol], $Au_{102}$(p-MBA)$_{44}$ and Au ~ $_{250}$(p-MBA) [MBA – mercaptobenzoic acid]), and remarkable control over the obtained superstructure sizes was achieved.[7,8] However, the emergence of new optical features within atomically-precise aggregates still remains poorly understood.

GNCs present an impressive level of core size and ligand-dependent fine-tuning of optical properties, also in the nonlinear optics regime.[9–11] Numerous cluster systems have been reported to have high two-photon absorption (2PA) cross-sections, making them interesting alternatives to organic dyes or other nanoparticles. For instance $Au_{25}(SR)_{18}$ (where SR – captopril) is characterized by two-photon absorption cross-sections reaching ~25 000 GM (the Goeppert–Mayer unit, 1 GM = $10^{-50}$ cm$^4$ s$^{-1}$).[12] Overall, the nonlinear optical properties of GNCs are structure-dependent and the concept of a "multi-shell system" composed of a metallic core and metal–ligand interface as well as surface ligand molecules is useful in interpreting them.[13] The aforementioned structural components of GNCs may communicate with each other by electronic charge transfer, which may result in high transition dipole moments, and thus elevated two-photon absorption cross-sections are expected. Efficient two-photon absorption of GNCs

[a] Institute of Advanced Materials, Wroclaw University of Science and Technology, Wybrzeże Wyspiańskiego 27, 50-370 Wroclaw, Poland. E-mail: Joanna.olesiak-banska@pwr.edu.pl
[b] Department of Physical Chemistry, University of Geneva, 30 Quai Ernest-Ansermet, 1211 Geneva 4, Switzerland

† Electronic supplementary information (ESI) available. See DOI: https://doi.org/10.1039/d4tc01698j

was reported, but no work has been done in terms of nonlinear optical characterization of GNC oligomers and superstructures which, due to the structural similarities, have the potential to compete with the best two-photon absorbers, such as organometallic dendrimers.[14] So far, however, the lack of data in the literature on nonlinear optical properties of atomically-precise nanoclusters and superstructures persists as a limiting factor for the development of novel applications in the field of optoelectronics, sensing and photonic technologies.[15,16]

Herein, we focus on the determination of two-photon absorption cross sections of atomically-precise $[Au_{25}(PET)_{18}]^0$ covalently linked with bidentate dithiol ((1*R*,1′*R*)-6,6′-(1,4-phenylene)di-1,1′-binaphthyl-2,2′-dithiol (diBINAS)) into dimers and trimers. Some of us have recently shown that nanoclusters connected with a diBINAS linker formed very stable oligomers thanks to the bidentate nature of the linker.[17] We show that covalent linking of atomically-precise gold nanoclusters leads to relatively weak modification of one-photon optical properties, but has a significant impact on two-photon properties. The two-photon spectra of the superstructures do not correspond to the simple sum of properties of the $[Au_{25}(PET)_{18}]^0$ building blocks: shifts and enhancements of the two-photon absorption cross section maxima are observed.

## Results and discussion

The $[Au_{25}(PET)_{18}]$ GNCs at 0 oxidation state were synthesized and linked into oligomers with bidentate dithiol, namely (1*R*,1′*R*)-6,6′-(1,4-phenylene)di-1,1′-binaphthyl-2,2′-dithiol (diBINAS), according to the protocol described by Świerczewski *et al.*[17] Herein, three separated cluster species will be discussed (see Fig. 1a), *i.e.*: monomer – $[Au_{25}(PET)_{18}]^0$, dimer – $[Au_{25}(PET)_{16}]^0$-diBINAS-$[Au_{25}(PET)_{16}]^0$, and $[Au_{25}(PET)_{16}]^0$-diBINAS-$[Au_{25}(PET)_{14}]^0$-diBINAS-$[Au_{25}(PET)_{16}]^0$ – trimer, all of them studied as solutions in toluene. Due to their dimensions being comparable to the Fermi wavelength of electrons in gold (<2 nm),[18] the nanoclusters are characterized by distinct molecular-like electronic transitions. For $[Au_{25}(PET)_{18}]^0$, characteristic absorption bands are located at 3.1 eV, 2.7 eV and 1.8 eV[19,20] (see Fig. 1b). The atomically-precise nature of our samples is also confirmed with MALTI-TOF MS measurements, where characteristic peaks at 7391 and 6055 *m*/*z* were found and assigned to the molecular peaks of $Au_{25}PET_{18}$ and $Au_{21}PET_{14}$. The latter is a typical fragment after loss of $Au_4PET_4$. In the case of oligomers, peaks characteristic of the terminal moiety (*i.e.* $-Au_{25}-PET_{16}-$) were identified for dimers, as well as for trimers with the addition of signals arising from the $-Au_{25}PET_{14}-$ central building block.[17]

Distinctive structural changes arising due to the diBINAS bridging of $[Au_{25}(PET)_{18}]^0$ units are manifested in the one-photon absorption spectra of the oligomers. Upon the formation of oligomers, the electronic transitions of $[(Au_{25}(PET)_{18}]^0$ in the 1.6–3.1 eV range become less intense, as shown in Fig. 1b. This can be explained by the reduction of the cluster symmetry, as the presence of multiple possible structural oligomeric isomers broadens and shifts the corresponding absorption features. Moreover, new electronic excited states

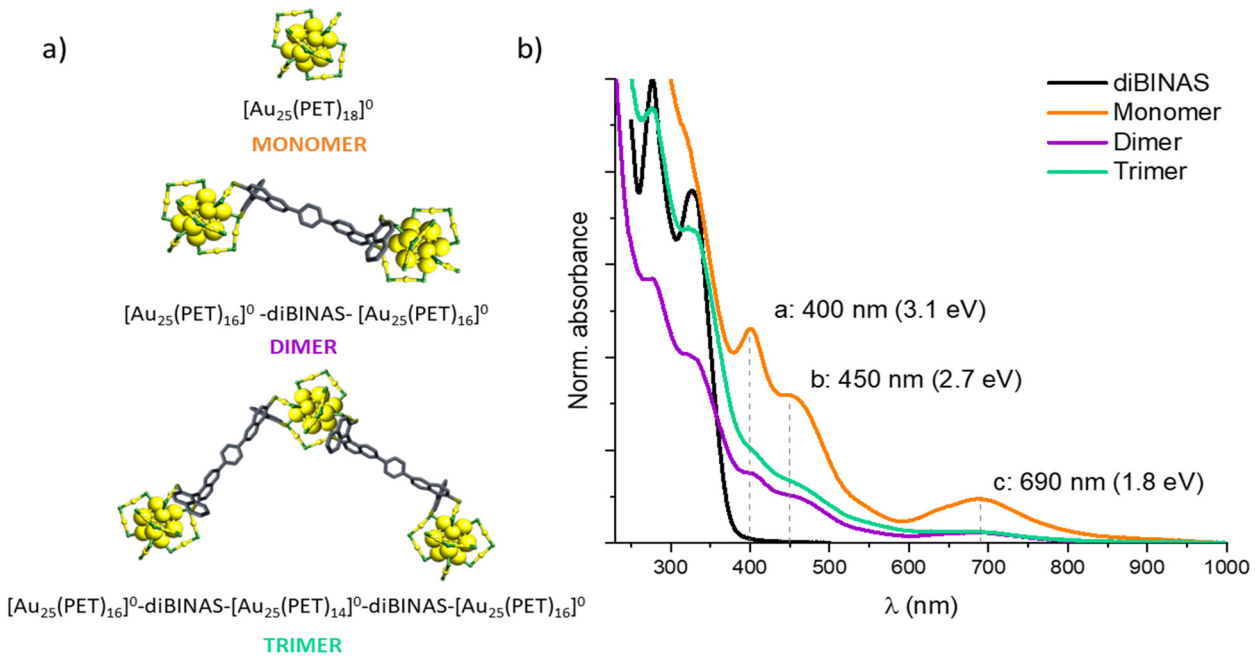


Fig. 1 (a) Simplified structures of the $[Au_{25}(PET)_{18}]^0$ monomer, dimer, and trimer depicted with corresponding color code: yellow – gold atoms, green – sulfur atoms, grey – carbon atoms (from diBINAS). PET (2-phenylethanethiol) ligands are omitted for clarity. The structures presented herein are not optimized and are included for illustrative purposes only. (b) Normalized optical absorption spectra of the corresponding structures: black line – diBINAS, orange line – monomer, purple line – dimer, green line – trimer, as measured in toluene. Characteristic electronic transitions are marked with dotted lines: a – 400 nm (3.1 eV), b – 450 nm (2.7 eV) and c – 690 nm (1.8 eV).

 

might appear due to metal–ligand interactions, thus contributing to broadening of the existing bands. As described in our previous work,[17] the $Au_{25}$-linker-$Au_{25}$ unit length is 3.28 ± 0.37 nm and 3.15 ± 0.35 nm for the dimer and trimer, respectively. The cluster's core-to-core distance was reported to be in the 2.0–2.2 nm range. Moreover, TEM imaging of trimers showed that a trigonal orientation of nanoclusters is possible. Among the aforementioned structures, trimers are characterized by a unique central building block, namely a nonterminal $-[Au_{25}PET_{14}]^0-$ moiety. On the other hand, the dimers are composed solely of two terminal $-[Au_{25}–PET_{16}]^0-$ units (see Fig. 1a). Therefore, the ligand shell of the trimers is expected to be rigidified, in contrast to the dimeric, and even more profoundly rigidified in comparison to the monomeric $[Au_{25}(PET)_{18}]^0$. Thus, nonradiative relaxation is moderated due to the incorporation of a bulky bidentate dithiol ligand, which enhances the dimer and trimer quantum yields (registered for a 370 nm excitation) by the factor, respectively, of 12 and 50.[17]

Herein, we discuss the influence of gold nanoclusters bridging with diBINAS into oligomers on their nonlinear optical properties. The nonlinear optical property, *i.e.* the two-photon absorption cross-section ($\sigma_2$), of the gold nanocluster monomer, dimer and trimer were determined with the z-scan technique for the 600–1500 nm spectral range. Detailed descriptions of the z-scan measurement procedure and calculation of the two-photon absorption cross-sections are described in the ESI.†[21,22] Exemplary open-aperture (OA) z-scan traces of the nanoclusters and their multimers are presented in Fig. 2 (additional OA and closed-aperture (CA) z-scan traces, including 3 mm silica reference, are also available in Fig. S1 and S2 (ESI†), respectively).

Fig. 3 incorporates the 1PA spectra plotted against the double wavelength, which is useful to assess whether a 2PA transition leads to a state that is also reachable by a 1PA transition. In the present case, the 2PA spectral characteristics of the monomer (red lines and points with error bars) do not match those of the 1PA spectrum (orange lines), but this is actually what may be expected for the centrosymmetric structure of the $Au_{25}(PET)_{18}$ nanocluster[19,23] since in the case of the presence of the center of symmetry, one- and two-photon allowed transitions are mutually exclusive. For dimers and trimers, we do observe a better overlap between the 2PA spectra and the corresponding 1PA bands plotted at the doubled wavelength (Fig. 3(b) and (c)). As only a small fraction of possible conformers may have a center of inversion, transitions to the new electronic excited states that will appear upon dimer/trimer formation should be symmetry allowed in both one- and two-photon absorption spectra. However, for oligomers (*i.e.* dimers and trimers), the chromophore may weakly perturb local transitions corresponding to ''monomeric'' dark states and thus symmetry relaxation will be weak (on passing from a monomer to a dimer or trimer).

A common feature of the 2PA spectra presented in Fig. 3a–c is a strong two-photon absorption for wavelengths <900 nm. Significant one-photon absorption is still present in this spectral range, which can largely influence the values of $\sigma_2$ in the range 600–900 nm through resonant enhancement or by contribution from excited state absorption. The changes of two-photon cross-section values are qualitatively similar for all the samples; however, quantitatively they are more pronounced for the dimer and trimer, especially for the band at ~690 nm. One possible explanation could be the strong 1PA of the diBINAS linker around 340 nm (compare to Fig. 1b, black curve) giving rise to two-photon absorption around 680 nm, so the neighboring spectral features in the 2PA spectra of the nanoclusters would exhibit smaller relative intensities (see pronounced new bands in the 1PA spectra of dimer and trimer ~340 nm). However, the electronic-structure calculations demonstrated that 2PA transition to a bright 1PA state at 340 nm of the isolated diBINAS linker is weak (see Table S1 in the ESI†), thus ruling out this possibility.

The 2PA spectra of the dimer and trimer show a significant drop of $\sigma_2$ at the wavelength ~700 nm, corresponding to the maximum of their lowest absorption band. Careful analysis of z-scan traces revealed that the contribution of saturable one-photon absorption (SA), which acts opposite to two-photon absorption, influences the nonlinear absorption effects at these wavelengths (see Fig. S3 (ESI†), and fitting procedure description). Similar effects were described in the previous studies on 2PA of gold $Au_{25}$ nanoclusters.[12,24]

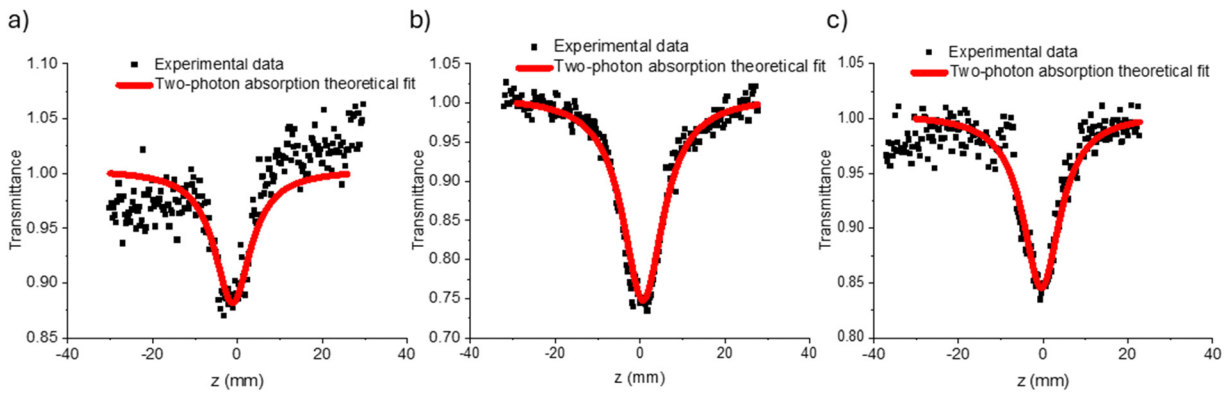


Fig. 2 Exemplary open-aperture (OA) z-scan traces assigned to the two-photon absorption phenomenon, as registered at 825 nm excitation for $[Au_{25}(PET)_{18}]^0$ (a) monomer, (b) dimer, and (c) trimer (linked by bidentate dithiol (diBINAS) and measured in toluene under 255 GW $cm^{-2}$ laser illumination).

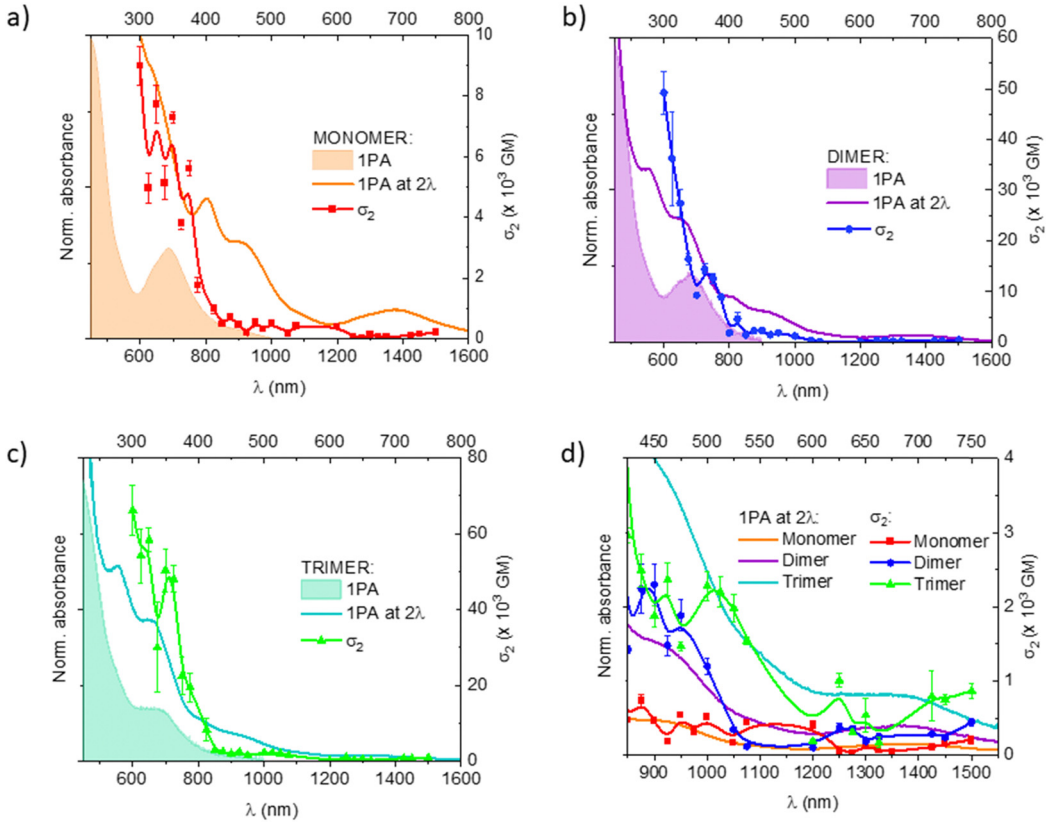


Fig. 3 Two-photon absorption cross sections ($\sigma_2$) – of the (a) monomer (red line and points), (b) dimer (blue line and points) and (c) trimer (green line and points) of $[Au_{25}(PET)_{18}]^0$. Simultaneously, one-photon absorption spectra are presented at 1PA wavelength and at twice the wavelength with orange, violet and mint shades and lines. Panel (d) compares the $\sigma_2$ curves in the out-of-resonance region (in reference to 1PA).

High values of $\sigma_2$ for all three samples are registered upon resonant excitation in the 1PA absorption range. The corresponding $\sigma_2$ values, presented herein, are comparable with other nanocluster systems composed of 25 atoms, *e.g.* water-soluble glutathione-stabilized ones or as measured in thin films.[25,26] The general overview of the $\sigma_2$ values registered for gold nanoclusters is available in the ESI† (see Table S2). Thus, we indicate that cluster oligomerization might be a new route to boost the nonlinear response of atomically-precise structures. For the monomer, dimer and trimer the $\sigma_2$ values at 600 nm are equal to $\sim$9000 $\pm$ 600 GM, 50 000 $\pm$ 4000 GM and 66 000 $\pm$ 6500 GM, respectively. Previous reports on the NLO properties of gold nanoclusters suggest that a one-photon double-resonance effect could lead to the large 2PA cross-sections observed experimentally.[27,28] We indicate that due to the complex nature of electronic states available for most of the atomically-precise gold nanocluster systems (usually expanding over the entire UV-vis wavelength range), it is challenging to unambiguously assign detected nonlinearities to two-photon absorption solely and detailed time-resolved studies will be beneficial to determine the contribution of excited states in the process.

In order to assess the effect of resonance enhancement of the two-photon absorption cross section, we invoke the quantum mechanical expressions defining purely molecular two-photon absorption transition matrix $S$ from the ground state 0 to an excited state $f$:

$$S_{ab} = \sum_n \left[ \frac{\langle 0|\hat{\mu}_a|n\rangle\langle n|\hat{\mu}_b|f\rangle}{\omega_{n0} - \frac{\omega_{f0}}{2}} + \frac{\langle 0|\hat{\mu}_b|n\rangle\langle n|\hat{\mu}_a|f\rangle}{\omega_{n0} - \frac{\omega_{f0}}{2}} \right] \quad (1)$$

where $\langle i|\hat{\mu}_a|j\rangle$ is the electronic transition moment operator between states $i$ and $j$. The summation runs over all excited states, from the ground to the final state. In the case of linearly polarized light, the two-photon absorption strength for an isotropic sample can then be expressed as:[29,30]

$$\langle \delta^{2PA} \rangle = \frac{1}{15} \sum_{ab} \left( S_{aa} S_{bb}^* + 2 S_{ab} S_{ba}^* \right) \quad (2)$$

Finally, the two-photon absorption cross section is proportional to $\langle \delta^{2PA} \rangle$:

$$\sigma_2 = \frac{(2\pi)^3 \alpha a_0^5 \omega^2}{c\pi L} \delta^{2PA} \quad (3)$$

where $\alpha$ is the fine structure constant, $a_0$ is the Bohr radius, $\omega$ is the frequency corresponding to the photon energy (half of the transition energy). The symbol $L$ refers to Lorentzian broadening, arising from the distribution of electron movement in high electric fields and typically equal to 0.1–0.2 eV.

 

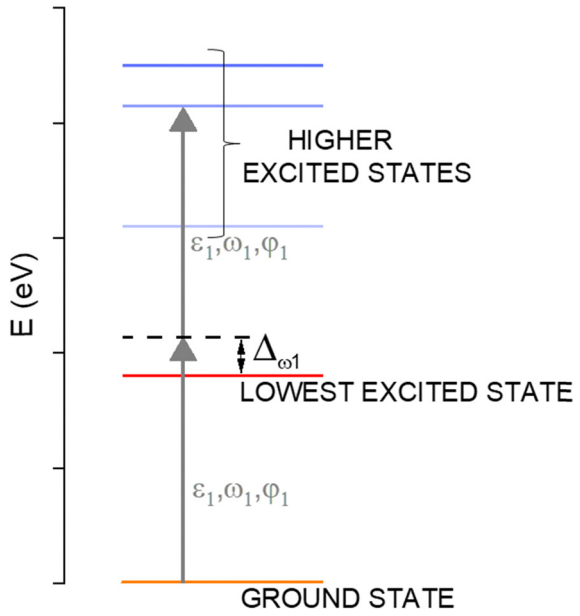


Fig. 4 Schematic energy diagram of two-photon excitation and the corresponding detuning factor ($\Delta$). For the $[Au_{25}(PET)_{18}]^0$ monomer, the lowest excited state lies at 1.8 eV (690 nm), and the excitation is shown at 650 nm ($\omega_1$).

The analysis of the two-photon transition matrix $S_{ab}$ might be helpful in understanding the 2PA strength in systems studied herein. In particular, the expression can be rewritten with an angular term between transition moment vectors taken into account.[31] It follows from the definition of $S_{ab}$ that when the angular frequency of a photon ($\omega_{f0}/2$) in the 2PA process approaches the energy difference between one of the excited states and the ground state ($\omega_{n0}$), there is a resonance enhancement of the two-photon response ($1/2\omega_{f0}-\omega_{n0}$ is also referred to as the detuning factor, $\Delta$, see Fig. 4). In fact, one finds enhanced 2PA cross sections around 600 nm. This can be explained by a small value of the detuning factor, $\Delta$, as the photon wavelength in a two-photon experiment equal to ~600 nm approaches a one-photon allowed state with maximum at 690 nm. The energy difference in the denominator of eqn (1) is one of the factors determining the 2PA response. Although $Au_{25}$ cores are found to be non-communicating electronically,[17] they might still be influenced by the diBINAS linker characterized by the lowest excited state near ~335 nm, corresponding to the energy from two photons.

As can be seen in Table 1, quantitatively, oligomerization of $[Au_{25}(PET)_{18}]^0$ with diBINAS strongly enhances the $\sigma_2$ values over the entire 600–1500 nm spectral range.

In the resonance wavelength range, the $\sigma_2$ is ~4 and ~8 times stronger than $\sigma_2$ of the monomer, for the dimer and trimer, respectively. On the other hand, in the "off resonance" part of the spectra, the enhancement factor is much lower, but still the $\sigma_2$ values of the dimers and trimers are larger than doubled and tripled $\sigma_2$ values in comparison to the monomer $[Au_{25}(PET)_{18}]^0$. It should be highlighted that the 2PA cross section enhancement may be due to both changes in the transition dipole moments and relative location of the first and higher excited states, which may strongly influence the resonance conditions (detuning factor). Thus, even though the changes observed in the one-photon absorption upon oligomerization of nanoclusters with diBINAS are moderate, they may result in significant differences in the enhancement on passing from monomer to dimer/trimer, as presented in Table 1.

Table 1 Enhancement factor ($F_n$) of $[Au_{25}(PET)_{18}]^0$ dimers ($n$ = 2) and trimers ($n$ = 3), calculated as: $F_2 = \sigma_2$ dimer/($\sigma_2$ monomer) or $F_3 = \sigma_2$ trimer/($\sigma_2$ monomer)

| Wavelength | Energy | Enhancement factor ($F_n$) | |
|---|---|---|---|
| nm | eV | $n$ = 2 | $n$ = 3 |
| 600 | 2.0 | 5.5 | 7.4 |
| 700–725 | 1.71–1.77 | 3.8[a] | 8.2[a] |
| 825 | 1.50 | 4.7 | 8.5 |
| 1000 | 1.24 | 2.3 | 4.5 |

[a] For wavelengths where the SA contribution is not present (compare with ESI, Fig. S1 and S3)

Linking of $Au_{25}$ GNCs with the diBINAS molecule may contribute strongly to the observed 2PA characteristics. As diBINAS presents an extended π-conjugation system, it might contribute to the electron delocalization within the entire superstructure system.[32] Even when the oligomer cluster to cluster distance does not allow for electronic communication between the GNC cores,[17] their electronic structure may be influenced by diBINAS. It should be noted that, while the $[Au_{25}(PET)_{18}]$ monomer has a radical character (it contains a half-filled orbital), the system of two GNC cores linked by diBINAS is a biradical. Biradical systems, however, with no metal centers, are already known to be superior in NLO response to corresponding radical equivalents.[33] Independent charge redistribution between two $[Au_{25}(PET)_{16}]^0$ terminating moieties and a single diBINAS molecule may be responsible for high enhancement factors for dimers, especially below 900 nm, where the lowest excited states of the diBINAS linker as well as one of the gold cores are near to the energy provided *via* simultaneous absorption of two photons. As early as in 1999, Chung *et al.*[34] showed that multi-branched organic structures linked together by a common center exhibit cooperative enhancement of 2PA and, at the same time, a similar enhancement was found for organometallic dendrimers.[35] In the present case, for trimers, state of the art levels of enhancement factors over the entire wavelength range might also be attributed to the cooperative enhancement effects observed for multi-branched structures.[9,13] Further theoretical work should be performed to establish the factors responsible for NLO enhancement in dithiol linked atomically-precise nanoclusters.

## Conclusions

We conclude that, even as covalent linking of $[Au_{25}(PET)_{18}]^0$ with diBINAS into oligomers leads to relatively small modification of the one-photon absorption spectra, their corresponding nonlinear optical properties are greatly enhanced. We show that in the one-photon resonant spectral region (*i.e.* below 900 nm) the

two-photon absorption cross section can reach the state of the art range values of 50 000 GM and 66 000 GM (at 600 nm) for dimers and trimers, respectively, in comparison to 9000 GM determined for the monomer. The relative values are thus very different from a simple additive scheme being enhanced by factors ~4 and ~8 for the dimer and the trimer, respectively. In the off-resonance spectral region, the trimers exhibit 4 times higher two-photon absorption cross-section values than the monomers, while the dimers are characterized by an enhancement factor slightly larger than 2. Additionally, we showed that two-photon transitions to bright one-photon states of the isolated diBINAS linker are weak, and thus quantitative changes of the two-photon absorption cross-sections between the oligomers and linker-free monomer are not governed by 2PA of the linker. A possible factor contributing to the nonlinear optical properties enhancement can be charge delocalization within the frames of $[Au_{25}(PET)_{16}]^0$-diBINAS terminal units. Therefore, the nanocluster core number or gold–sulfur staple-like motif alteration might be crucial to design efficient and functional multiphoton absorbers composed of atomically-precise gold nanocluster subunits. Our results contribute to a better understanding of GNCs' nonlinear optical properties, as well as open up new pathways for the design of atomically-precise superstructures with superior nonlinear optical performance.

## Author contributions

P. Obstarczyk prepared samples, measured and calculated two-photon absorption cross-sections of gold nanoclusters, analyzed the data, and prepared the original draft of the manuscript. J. Osmólska performed control z-scan experiments and initial fitting. M. Swierczewski and T. Bürgi synthesized, purified, and separated the gold nanoclusters and corresponding diBINAS-linked superstructures. M. Samoć supervised the conceptualization of the original draft and discussion. J. Olesiak-Bańska formulated the research goals, supervised the research, analyzed the data and acquired the funding. All authors took part in writing and editing the manuscript.

## Data availability

The authors confirm that the data supporting the findings of this study are available within the article and/or its ESI.† Additional data that support the findings of this study are available on request from the corresponding author JOB.

## Conflicts of interest

There are no conflicts to declare.

## Acknowledgements

This work was supported by the National Science Centre (Poland) under the Sonata Bis project (2019/34/E/ST5/00276). PO acknowledges the support from the Foundation for Polish Science (FNP) within the frame of the START program. We thank prof. Robert Zaleśny for DFT calculations and discussions.

## Notes and references

1 M. Grzelczak, J. Vermant, E. M. Furst and L. M. Liz-Marzán, Directed Self-Assembly of Nanoparticles, *ACS Nano*, 2010, **4**, 3591–3605.
2 N. J. Halas, S. Lal, W.-S. Chang, S. Link and P. Nordlander, Plasmons in Strongly Coupled Metallic Nanostructures, *Chem. Rev.*, 2011, **111**, 3913–3961.
3 K. Deng, Z. Luo, L. Tan and Z. Quan, Self-Assembly of Anisotropic Nanoparticles into Functional Superstructures, *Chem. Soc. Rev.*, 2020, **49**, 6002–6038.
4 R. Jin, Atomically Precise Metal Nanoclusters: Stable Sizes and Optical Properties, *Nanoscale*, 2015, **7**, 1549–1565.
5 I. Chakraborty and T. Pradeep, Atomically Precise Clusters of Noble Metals: Emerging Link between Atoms and Nanoparticles, *Chem. Rev.*, 2017, **117**, 8208–8271.
6 E. Banach and T. Bürgi, Metal Nanoclusters as Versatile Building Blocks for Hierarchical Structures, *Helv. Chim. Acta*, 2022, **105**, e202100186.
7 A. Sels, G. Salassa, F. Cousin, L.-T. Lee and T. Bürgi, Covalently Bonded Multimers of Au25(Sbut)18 as a Conjugated System, *Nanoscale*, 2018, **10**, 12754–12762.
8 T. Lahtinen, E. Hulkko, K. Sokołowska, T.-R. Tero, V. Saarnio, J. Lindgren, M. Pettersson, H. Häkkinen and L. Lehtovaara, Covalently Linked Multimers of Gold Nanoclusters Au102(P-Mba)44 and Au ~ 250(P-Mba)N, *Nanoscale*, 2016, **8**, 18665–18674.
9 I. Russier-Antoine, F. Bertorelle, N. Calin, Ž. Sanader, M. Krstić, C. Comby-Zerbino, P. Dugourd, P.-F. Brevet, V. Bonačić-Koutecký and R. Antoine, Ligand-Core NloPhores: A Combined Experimental and Theoretical Approach to the Two-Photon Absorption and Two-Photon Excited Emission Properties of Small-Ligated Silver Nanoclusters, *Nanoscale*, 2017, **9**, 1221–1228.
10 J. Olesiak-Banska, M. Waszkielewicz, P. Obstarczyk and M. Samoc, Two-Photon Absorption and Photoluminescence of Colloidal Gold Nanoparticles and Nanoclusters, *Chem. Soc. Rev.*, 2019, **48**, 4087–4117.
11 A. Pniakowska, K. Kumaranchira Ramankutty, P. Obstarczyk, M. Perić Bakulić, Ž. Sanader Maršić, V. Bonačić-Koutecký, T. Bürgi and J. Olesiak-Bańska, Gold-Doping Effect on Two-Photon Absorption and Luminescence of Atomically Precise Silver Ligated Nanoclusters, *Angew. Chem., Int. Ed.*, 2022, **61**, e202209645.
12 J. Olesiak-Banska, M. Waszkielewicz, K. Matczyszyn, M. Samoc and A. Closer Look, at Two-Photon Absorption, Absorption Saturation and Nonlinear Refraction in Gold Nanoclusters, *RSC Adv.*, 2016, **6**, 98748–98752.
13 V. Bonačić-Koutecký and R. Antoine, Enhanced Two-Photon Absorption of Ligated Silver and Gold Nanoclusters: Theoretical and Experimental Assessments, *Nanoscale*, 2019, **11**, 12436–12448.

 

14 R. L. Roberts, T. Schwich, T. C. Corkery, M. P. Cifuentes, K. A. Green, J. D. Farmer, P. J. Low, T. B. Marder, M. Samoc and M. G. Humphrey, Organometallic Complexes for Nonlinear Optics. 45. Dispersion of the Third-Order Nonlinear Optical Properties of Triphenylamine-Cored Alkynylruthenium Dendrimers, *Adv. Mater.*, 2009, **21**, 2318–2322.
15 J.-r Choi, D.-M. Shin, H. Song, D. Lee and K. Kim, Current Achievements of Nanoparticle Applications in Developing Optical Sensing and Imaging Techniques, *Nano Converg.*, 2016, **3**, 30.
16 B. Fu, *et al.*, Recent Progress on Metal-Based Nanomaterials: Fabrications, Optical Properties, and Applications in Ultrafast Photonics, *Adv. Funct. Mater.*, 2021, **31**, 2107363.
17 M. Swierczewski, *et al.*, Exceptionally Stable Dimers and Trimers of Au25 Clusters Linked with a Bidentate Dithiol: Synthesis, Structure and Chirality Study, *Angew. Chem., Int. Ed.*, 2023, **62**, e202215746.
18 X. Kang, H. Chong and M. Zhu, Au25(Sr)18: The Captain of the Great Nanocluster Ship, *Nanoscale*, 2018, **10**, 10758–10834.
19 M. Zhu, C. M. Aikens, F. J. Hollander, G. C. Schatz and R. Jin, Correlating the Crystal Structure of a Thiol-Protected Au25 Cluster and Optical Properties, *J. Am. Chem. Soc.*, 2008, **130**, 5883–5885.
20 M. A. Tofanelli, K. Salorinne, T. W. Ni, S. Malola, B. Newell, B. Phillips, H. Häkkinen and C. J. Ackerson, Jahn–Teller Effects in Au25(Sr)18, *Chem. Sci.*, 2016, **7**, 1882–1890.
21 M. Samoc; A. Samoc; G. Dalton; M. Cifuentes; M. Humphrey and P. Fleitz, *Two-Photon Absorption Spectra and Dispersion of the Complex Cubic Hyperpolarizability* Γ *in Organic and Organometallic Chromophores*. 2011; pp. 341–355.
22 M. Samoc, A. Samoc, B. Luther-Davies, M. G. Humphrey and M.-S. Wong, Third-Order Optical Nonlinearities of Oligomers, Dendrimers and Polymers Derived from Solution Z-Scan Studies, *Opt. Mater.*, 2003, **21**, 485–488.
23 M. Zhu, W. T. Eckenhoff, T. Pintauer and R. Jin, Conversion of Anionic [Au25(Sch2ch2ph)18]− Cluster to Charge Neutral Cluster Via Air Oxidation. *The*, *J. Phys. Chem. C*, 2008, **112**, 14221–14224.
24 Z. Su, M. Bejide, P. Ferrari, K. A. Kaw, M. Moris, K. Clays, S. Knoppe, P. Lievens and E. Janssens, The Wavelength-Dependent Non-Linear Absorption and Refraction of Au25 and Au38 Monolayer-Protected Clusters, *Nanoscale*, 2022, **14**, 3618–3624.
25 R. Ho-Wu, P. K. Sahu, N. Wu, T. K. Chen, C. Yu, J. Xie and T. Goodson, Understanding the Optical Properties of Au@Ag Bimetallic Nanoclusters through Time-Resolved and Nonlinear Spectroscopy. *The*, *J. Phys. Chem. C*, 2018, **122**, 24368–24379.
26 R. Ho-Wu, S. H. Yau and T. Goodson, Linear and Nonlinear Optical Properties of Monolayer-Protected Gold Nanocluster Films, *ACS Nano*, 2016, **10**, 562–572.
27 Z. Hu and L. Jensen, Importance of Double-Resonance Effects in Two-Photon Absorption Properties of Au25(Sr)18−, *Chem. Sci.*, 2017, **8**, 4595–4601.
28 G. Yousefalizadeh, S. Ahmadi, N. J. Mosey and K. G. Stamplecoskie, Exciting Clusters, What Does Off-Resonance Actually Mean?, *Nanoscale*, 2021, **13**, 242–252.
29 P. R. Monson and W. M. McClain, Polarization Dependence of the Two-Photon Absorption of Tumbling Molecules with Application to Liquid 1-Chloronaphthalene and Benzene. *The*, *J. Chem. Phys.*, 2003, **53**, 29–37.
30 V. Bonačić-Koutecký, Theoretical Design of New Class of Optical Materials Based on Small Noble Metal Nanocluster-Biomolecule Hybrids and Its Potential for Medical Applications, *Adv. Phys. X*, 2017, **2**, 695–716.
31 M. T. P. Beerepoot, M. M. Alam, J. Bednarska, W. Bartkowiak, K. Ruud and R. Zaleśny, Benchmarking the Performance of Exchange-Correlation Functionals for Predicting Two-Photon Absorption Strengths, *J. Chem. Theory Comput.*, 2018, **14**, 3677–3685.
32 W. S. Compel, O. A. Wong, X. Chen, C. Yi, R. Geiss, H. Häkkinen, K. L. Knappenberger and C. J. Ackerson, Dynamic Diglyme-Mediated Self-Assembly of Gold Nanoclusters, *ACS Nano*, 2015, **9**, 11690–11698.
33 K. Kamada, *et al.*, Impact of Diradical Character on Two-Photon Absorption: Bis(Acridine) Dimers Synthesized from an Allenic Precursor, *J. Am. Chem. Soc.*, 2013, **135**, 232–241.
34 S.-J. Chung, K.-S. Kim, T.-C. Lin, G. S. He, J. Swiatkiewicz and P. N. Prasad, Cooperative Enhancement of Two-Photon Absorption in Multi-Branched Structures. *The*, *J. Phys. Chem. B*, 1999, **103**, 10741–10745.
35 A. M. McDonagh, M. G. Humphrey, M. Samoc and B. Luther-Davies, Organometallic Complexes for Nonlinear Optics. 17.1 Synthesis, Third-Order Optical Nonlinearities, and Two-Photon Absorption Cross Section of an Alkynylruthenium Dendrimer, *Organometallics*, 1999, **18**, 5195–5197.